

Inositol hexakisphosphate suppresses excitatory neurotransmission via synaptotagmin-1 C2B domain in the hippocampal neuron

Shao-Nian Yang^{a,b,1,2}, Yue Shi^{a,1}, Guang Yang^a, Yuxin Li^b, Lina Yu^a, Ok-Ho Shin^d, Taulant Bacaj^c, Thomas C. Südhof^c, Jia Yu^a, and Per-Olof Berggren^a

^aThe Rolf Luft Research Center for Diabetes and Endocrinology, Karolinska Institutet, SE-171 76 Stockholm, Sweden; ^bNational Engineering Laboratory for Druggable Gene and Protein Screening, Northeast Normal University, Changchun 130024, China, ^cDepartment of Molecular and Cellular Physiology and Howard Hughes Medical Institute, Stanford University, Palo Alto, CA 94305-5453; and ^dDepartment of Neuroscience and Cell Biology, University of Texas Medical Branch, Galveston, TX 77555

Edited* by William A. Catterall, University of Washington School of Medicine, Seattle, WA, and approved June 12, 2012 (received for review September 13, 2011)

Inositol hexakisphosphate (InsP₆) levels rise and fall with neuronal excitation and silence, respectively, in the hippocampus, suggesting potential signaling functions of this inositol polyphosphate in hippocampal neurons. We now demonstrate that intracellular application of InsP₆ caused a concentration-dependent inhibition of autaptic excitatory postsynaptic currents (EPSCs) in cultured hippocampal neurons. The treatment did not alter the size and replenishment rate of the readily releasable pool in autaptic neurons. Intracellular exposure to InsP₆ did not affect spontaneous EPSCs or excitatory amino acid-activated currents in neurons lacking autapses. The InsP₆-induced inhibition of autaptic EPSCs was effectively abolished by coapplication of an antibody to synaptotagmin-1 C2B domain. Importantly, preabsorption of the antibody with a GST-WT synaptotagmin-1 C2B domain fragment but not with a GST-mutant synaptotagmin-1 C2B domain fragment that poorly reacted with the antibody impaired the activity of the antibody on the InsP₆-induced inhibition of autaptic EPSCs. Furthermore, K⁺ depolarization significantly elevated endogenous levels of InsP₆ and occluded the inhibition of autaptic EPSCs by exogenous InsP₆. These data reveal that InsP₆ suppresses excitatory neurotransmission via inhibition of the presynaptic synaptotagmin-1 C2B domain-mediated fusion via an interaction with the synaptotagmin Ca²⁺-binding sites rather than via interference with presynaptic Ca²⁺ levels, synaptic vesicle trafficking, or inactivation of postsynaptic ionotropic glutamate receptors. Therefore, elevated InsP₆ in activated neurons serves as a unique negative feedback signal to control hippocampal excitatory neurotransmission.

Ca²⁺ sensor | exocytosis | synaptic signal transduction | whole cell patch clamp recording

Inositol hexakisphosphate (InsP₆) is the most abundant inositol polyphosphate in cells and targets a number of specific InsP₆-binding proteins (1–5). Therefore, this inositol polyphosphate acts as a multifaceted player in cell signaling (1–10). The hippocampal neuron displays a higher rate of synthesis of InsP₆ and is equipped with more abundant InsP₆-binding proteins compared with other neurons (11, 12). InsP₆ levels rise and fall with neuronal excitation and silence, respectively, in the hippocampus (13). However, we do not know if this inositol polyphosphate is involved in hippocampal neurotransmission. The present work shows that intracellular InsP₆ inhibits excitatory neurotransmission via inhibition of Ca²⁺ triggering of presynaptic membrane fusion mediated by the synaptotagmin-1 C2B domain rather than by interference with synaptic vesicle trafficking or inactivation of postsynaptic ionotropic glutamate receptors. Such an InsP₆-mediated mechanism most likely functions as unique negative feedback machinery to control hippocampal excitatory neurotransmission.

Results

InsP₆ Inhibits Autaptic Excitatory Postsynaptic Currents in a Concentration-Dependent Manner. To determine if intracellular InsP₆ regulates excitatory neurotransmission, we examined changes in autaptic excitatory postsynaptic currents (EPSCs) in cultured hippocampal neurons following intracellular application of InsP₆ at concentrations ranging from 3 to 50 μM. These cultured hippocampal neurons form direct synaptic connections on themselves (i.e., autapses) (14). They serve as a simplified synaptic model allowing us to record EPSCs and introduce InsP₆ into presynaptic terminals in the same neuron by the same whole-cell patch-clamp electrode. As shown in Fig. 1, intracellular dialysis of standard intracellular solution in the absence of InsP₆ as a control ($n = 6$) did not significantly alter autaptic EPSCs evoked by low-frequency stimulation (once per minute) during 20 min. Intracellularly applied InsP₆ concentration-dependently inhibited autaptic EPSCs (Fig. 1). The effect became statistically significant when InsP₆ concentration reached 20 μM and higher ($n = 6$ at 20 μM and $n = 6$ at 50 μM; $P < 0.01$ vs. control) (Fig. 1). The IC₅₀ value of InsP₆ was estimated to be 14.4 μM. Moreover, neurons internally exposed to 50 μM inositol hexasulfate hexapotassium (InsS₆; $n = 8$), a structural analog of InsP₆, did not exhibit a significant reduction in autaptic EPSCs in comparison to control neurons (Fig. 1). This verifies that the inhibitory effect of InsP₆ on autaptic EPSCs is specific.

InsP₆ Reduces Autaptic EPSCs but Does Not Vary Readily Releasable Pool Size and Replenishment Rate. To localize where InsP₆ acted to reduce autaptic EPSCs, we evaluated if intracellular InsP₆ varies the size and replenishment rate of the readily releasable pool (RRP). These two important indexes were quantified by puffing 500 mM sucrose in excitatory autaptic hippocampal neurons. Fig. 2 *A* and *B* shows that intracellular application of 20 μM InsP₆ ($n = 16$) for 20 min significantly reduced autaptic EPSCs in comparison to that of standard intracellular solution ($n = 16$; $P < 0.01$). However, the treatment did not alter EPSC responses to hypertonic sucrose. There is no significant difference in the synaptic charge transfer integrated over the transient phase of sucrose-induced responses, reflecting RRP size (15, 16), between

Author contributions: S.-N.Y. and Y.S. designed research; S.-N.Y., Y.S., G.Y., Y.L., L.Y., O.-H.S., T.B., and J.Y. performed research; S.-N.Y. and Y.S. analyzed data; and S.-N.Y., T.C.S., and P.-O.B. wrote the paper.

Conflict of interest statement: P.-O.B. is the founder of the Biotech Company BioCrine AB and is also a member of the board of this company. S.-N.Y. is a consultant for BioCrine AB.

*This Direct Submission article had a prearranged editor.

¹S.-N.Y. and Y.S. contributed equally to this work.

²To whom correspondence should be addressed. E-mail: shao-nian.yang@ki.se.

This article contains supporting information online at www.pnas.org/lookup/suppl/doi:10.1073/pnas.1115070109/-DCSupplemental.

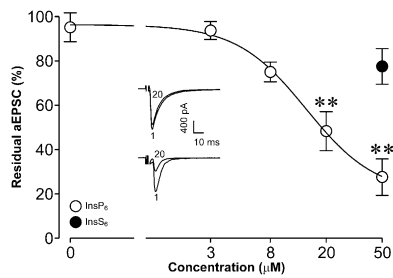


Fig. 1. Intracellular application of InsP₆ concentration-dependently reduces autaptic EPSCs (aEPSCs). The concentration–response curve for the InsP₆-induced inhibition of autaptic EPSCs shows that InsP₆ at concentrations of 20 and 50 µM ($n = 6$ for both) significantly reduces autaptic EPSCs compared with vehicle control ($n = 6$). However, InsS₆, a structural analog of InsP₆, produces a slight decrease in autaptic EPSCs at a concentration of 50 µM ($n = 8$) but without statistical significance. The IC₅₀ value of InsP₆ is 14.4 µM. (Insets) Sample autaptic EPSC traces recorded in a control neuron (Upper) and a neuron internally exposed to 50 µM InsP₆ (Lower) are shown. Numbers indicate the time (min) when autaptic EPSCs are registered after forming the whole-cell configuration. ** $P < 0.01$ vs. control. pA, picoampere.

control neurons and neurons internally exposed to 20 µM InsP₆ (Fig. 2 C and D). Furthermore, intracellular exposure to this inositol polyphosphate induced no significant change in cumulative charge transfer integrated over 1-s bins in response to a 15-s challenge with hypertonic sucrose compared with that to standard intracellular solution (Fig. 2E). The initial fast decay phase and very slow second decay phase reflect the release rate and replenishment rate of the RRP, respectively (16, 17). Both are similar between control neurons and InsP₆-exposed neurons (Fig. 2E). These data reveal that intracellular InsP₆ reduces autaptic EPSCs by bypassing regulatory processes of RRP size and replenishment rate, and suggest that it may act at post-synaptic ionotropic glutamate receptors and/or the final step of exocytosis, namely, fusion at presynaptic terminals.

InsP₆ Alters Neither Spontaneous EPSCs Nor Excitatory Amino Acid-Activated Currents. To discriminate between the postsynaptic and presynaptic effect of InsP₆ in autapses, spontaneous EPSCs in neurons lacking autapses were analyzed in the presence ($n = 10$) or absence ($n = 9$) of 20 µM InsP₆. Spontaneous EPSCs recorded in neurons filled with InsP₆ resembled those in control neurons (Fig. 3A). Detailed quantitative analysis of spontaneous EPSCs showed that profiles of the cumulative charge transfer integrated over 1-min bins during 20 min were similar between control neurons and InsP₆-treated neurons (Fig. 3A). The data suggest that intracellular InsP₆ does not act on postsynaptic ionotropic glutamate receptors to inhibit EPSCs.

To confirm the absence of a postsynaptic action of InsP₆ on EPSCs, effects of this inositol polyphosphate on the excitatory amino acid-activated currents were examined in neurons without autapses. As shown in Fig. 3 B–E, the density of whole-cell currents evoked by the nonselective glutamate receptor agonist glutamate (Fig. 3B) and the selective ionotropic glutamate receptor agonists AMPA (Fig. 3C), NMDA (Fig. 3D), and kainate (Fig. 3E) did not differ in the presence or absence of intracellular InsP₆. These data exclude the possibility for intracellular InsP₆ to suppress EPSCs via inhibition of postsynaptic ionotropic glutamate receptors and verify that InsP₆ applied in the hippocampal neuron with autapses acts at presynaptic components to suppress excitatory neurotransmitter release.

InsP₆ Suppresses Autaptic EPSCs via the Synaptotagmin-1 C2B Domain. The above data allowed us to narrow down InsP₆ target candidates to the final step of exocytosis, namely, fusion. We decided to investigate if the C2B domain of synaptotagmin-1, the

major Ca²⁺ sensor for fast synaptic vesicle exocytosis (18), mediates InsP₆ inhibition on autaptic EPSCs. To do so, we examined effects of intracellular application of a polyclonal rabbit antibody to synaptotagmin-1 C2B domain fragment (Anti-C2B; serum Y940) and GST–synaptotagmin-1 C2B domain fragment (19, 20) on the InsP₆-induced inhibition of autaptic EPSCs. Fig. 4 shows that Anti-C2B coapplied with InsP₆ (20 µM InsP₆/Anti-C2B, $n = 9$) significantly diminished the InsP₆-induced inhibition of autaptic EPSCs in comparison to InsP₆ plus nonimmune IgG (20 µM InsP₆/IgG, $n = 7$; $P < 0.01$). It is noteworthy that Anti-C2B ($n = 10$) only marginally reduced autaptic EPSCs in the absence of InsP₆ compared with nonimmune IgG ($n = 9$; $P = 0.054$) (Fig. 4). Importantly, preabsorption of Anti-C2B with GST-WT synaptotagmin-1 C2B domain fragment (GST-C2Bw) but not with GST-mutant

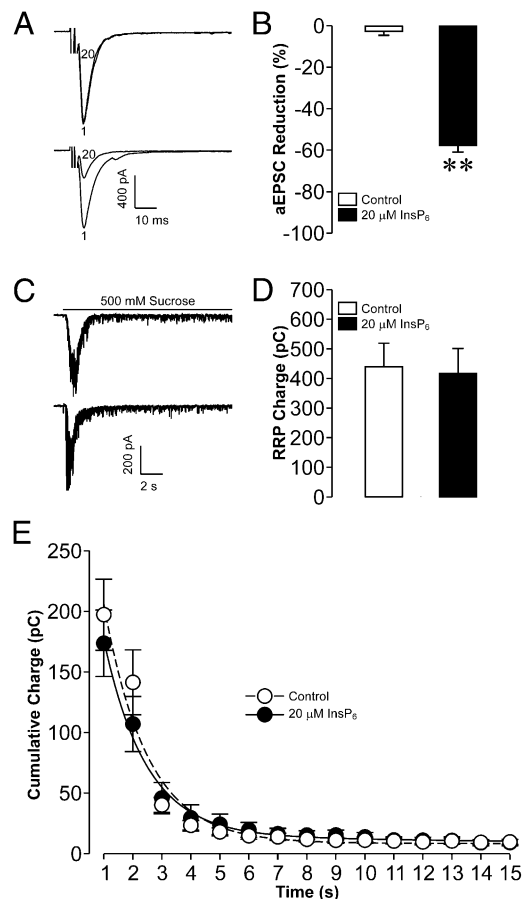


Fig. 2. Intracellular administration of InsP₆ decreases autaptic EPSCs but does not change the size and replenishment rate of the RRP. (A) Sample autaptic EPSC traces are registered in a control neuron (Upper) and in a neuron dialyzed with 20 µM InsP₆ (Lower). Numbers indicate the time (min) when autaptic EPSCs are registered after forming the whole-cell configuration. (B) Summary graph shows that neurons dialyzed with 20 µM InsP₆ ($n = 16$) exhibit a significant reduction in autaptic EPSCs in comparison to control neurons ($n = 16$). ** $P < 0.01$ vs. control. (C) Sample EPSC traces evoked by puffing 500 mM sucrose in a control autaptic neuron (Upper) and an autaptic neuron internally exposed to 20 µM InsP₆ (Lower) are shown. (D) Summary graph illustrates that the synaptic charge transfer integrated over the transient phase of sucrose-induced responses, reflecting RRP size, is similar in the absence ($n = 16$) and presence ($n = 16$) of 20 µM InsP₆. (E) Summary graph shows that there is no significant difference in cumulative charge transfer integrated over 1-s bins in response to a 15-s challenge with hypertonic sucrose between control autaptic neurons ($n = 16$) and InsP₆-exposed autaptic neurons ($n = 16$). The initial fast decay phase and very slow second decay phase reflect the release rate and replenishment rate of the RRP, respectively. pA, picoampere; pC, picocoulomb.

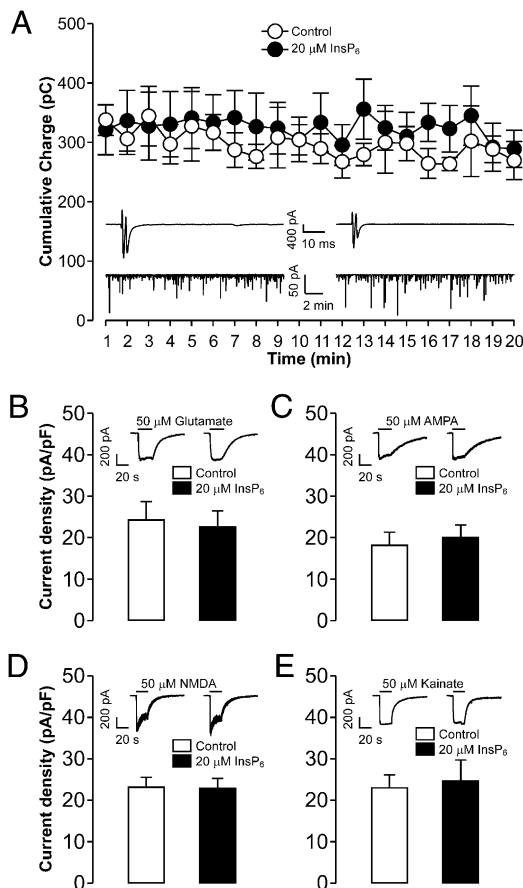


Fig. 3. Intracellular dialysis of InsP_6 causes no change in either spontaneous EPSCs or excitatory amino acid-activated currents. (A) Summary graph shows that neurons lacking autapses display similar profiles of the cumulative charge transfer integrated over 1-min bins, which is used to quantify spontaneous EPSCs, when dialyzed with vehicle control ($n = 9$) or $20 \mu\text{M}$ InsP_6 ($n = 10$). (Insets) Sample spontaneous EPSC traces recorded in a control neuron (Left Lower) and a neuron filled with $20 \mu\text{M}$ InsP_6 (Right Lower) are shown, with both only showing electrical stimulation artifacts (Upper) without autaptic EPSCs when subjected to depolarizing voltage pulses (2-ms duration, 80-mV amplitude). (B) There is no significant difference in the density of whole-cell currents induced by $50 \mu\text{M}$ glutamate between control ($n = 14$) and $20\text{-}\mu\text{M}$ InsP_6 -treated neurons ($n = 14$). (C) Density of whole-cell currents activated by $50 \mu\text{M}$ AMPA is similar between control neurons ($n = 13$) and neurons dialyzed with $20 \mu\text{M}$ InsP_6 ($n = 12$). (D) Density of whole-cell currents induced by $50 \mu\text{M}$ NMDA in control neurons ($n = 13$) does not significantly differ from that in $20\text{-}\mu\text{M}$ InsP_6 -exposed neurons ($n = 12$). (E) Density of whole-cell currents activated by $50 \mu\text{M}$ kainate in control neurons ($n = 13$) resembles that in neurons exposed to $20 \mu\text{M}$ InsP_6 ($n = 13$). (Insets) Sample glutamate- (B), AMPA- (C), NMDA- (D), and kainate- (E) activated current traces in a control neuron (Left) and an InsP_6 -exposed neuron (Right) are illustrated. pA, picoampere; pC, picocoulomb; pF, picofarad.

synaptotagmin-1 C2B domain fragment (GST-C2Bm) significantly ablated the effect of the antibody on the InsP_6 -induced inhibition of autaptic EPSCs. As shown in Fig. 4, a similar reduction in autaptic EPSCs occurred to $20 \mu\text{M}$ InsP_6 /Anti-C2B and $20 \mu\text{M}$ InsP_6 /Anti-C2B/GST-C2Bm ($n = 7$), but it is significantly less than that observed with $20 \mu\text{M}$ InsP_6 /Anti-C2B/GST-C2Bw ($n = 13$; $P < 0.01$). There are no significant differences in the InsP_6 -induced inhibition of autaptic EPSCs between $20 \mu\text{M}$ InsP_6 /Anti-C2B/GST-C2Bw, $20 \mu\text{M}$ InsP_6 /IgG, $20 \mu\text{M}$ InsP_6 /GST-C2Bm ($n = 14$), and $20 \mu\text{M}$ InsP_6 /GST-C2Bw ($n = 8$) (Fig. 4). Fig. 4 shows that a small rundown of autaptic EPSCs appeared in intracellular dialysis with IgG, GST-C2Bm ($n = 8$), GST-C2Bw ($n = 8$), and Anti-C2B/GST-C2Bw ($n = 11$), as

it did under internal exposure to standard intracellular solution as shown in Figs. 1, 2, and 5. These data reveal that intracellular InsP_6 inhibits autaptic EPSCs via the synaptotagmin-1 C2B domain.

It is puzzling that the mutant C2B domain was unable to nullify the mitigating effect of the C2B domain on the antibody's inhibition of InsP_6 because the C2B domain mutation changes only a single residue in the peptide epitope for the antibody (Fig. 4C). Thus, we confirmed by quantitative immunoblotting that the antibody reacts greater than fivefold less strongly with mutant than with WT C2B domain (Figs. 4D and E). Because the C2B domain mutation in the Y940 antibody epitope is in the top Ca^{2+} -binding loop 1 of the C2B domain (21), the antibody must react specifically with this site, suggesting that InsP_6 specifically acts via this sequence of the C2B domain.

K^+ Depolarization Elevates Endogenous Levels of InsP_6 and Occludes Inhibition of Exogenous InsP_6 on Autaptic EPSCs. To provide support for the physiological relevance of the exogenous InsP_6 -induced inhibition of EPSCs, we examined if endogenous levels of InsP_6 change in cultured hippocampal neurons following depolarization and also evaluated if endogenously generated InsP_6 did the same as exogenous InsP_6 . Fig. 5A shows that depolarization with 90 mM KCl for 1 min ($n = 6$) significantly elevated [^3H] InsP_6 levels in hippocampal cultures labeled with [^3H]inositol ($30 \mu\text{Ci}/\text{mL}$) for 3 d in comparison to nonstimulated neurons as a control ($n = 6$; $P < 0.01$). As demonstrated above, intracellular exposure to $20 \mu\text{M}$ InsP_6 ($n = 11$) induced a significant reduction in autaptic EPSCs compared with that to standard intracellular solution ($n = 11$; $P < 0.01$) (Fig. 5B and C). Importantly, prior K^+ depolarization significantly occluded inhibition of exogenous InsP_6 on autaptic EPSCs. The inhibition of exogenous InsP_6 on autaptic EPSCs in neurons subjected to prior K^+ depolarization ($n = 12$) is less than 50% of that observed in neurons without prior K^+ depolarization ($P < 0.01$) (Fig. 5C). Interestingly, an appreciable increase in autaptic EPSCs appeared in neurons internally dialyzed with standard intracellular solution in the absence ($n = 14$) and presence ($n = 13$) of $50 \mu\text{M}$ InsP_6 (Fig. 5C). This reflects that the endogenous InsP_6 -induced inhibition of EPSCs was released during washout of endogenously generated InsP_6 and confirms that intracellular exposure to $50 \mu\text{M}$ InsP_6 did not significantly influence autaptic EPSCs. These data demonstrate that endogenously generated InsP_6 does down-regulate EPSCs in the same way as exogenous InsP_6 does.

Discussion

The present study reveals that exogenous InsP_6 effectively inhibited autaptic EPSCs, reflecting excitatory neurotransmission, in a concentration-dependent manner when dialyzed into cultured hippocampal neurons. It provides a mechanistic picture of the InsP_6 -induced inhibition of hippocampal excitatory neurotransmission. It also demonstrates that the hippocampal neuron can indeed produce such a unique endogenous signaling molecule to control its excitatory neurotransmission.

The continued neurotransmitter release during prolonged stimulation relies on not only the sustained operation of synaptic vesicle exocytosis but the timely replenishment of synaptic vesicle pools (22–25). Both processes could be affected by InsP_6 to inhibit autaptic EPSCs evoked by sequential stimulation. The hypertonic sucrose shock is widely used to estimate RRP size and replenishment rate. This procedure destabilizes the active zone to release docked and fusion-competent vesicles in a Ca^{2+} -independent fashion, thereby reflecting the RRP that is regulated by Ca^{2+} (15, 26). For example, genetic ablation of the Ca^{2+} sensor synaptotagmin I dramatically reduces Ca^{2+} -evoked EPSCs but does not affect the hypertonic sucrose-induced EPSCs (18). This useful approach helped us localize InsP_6 targets in the autapse. Interestingly, autaptic neurons did display a significant reduction in their autaptic EPSCs but did not change their RRP

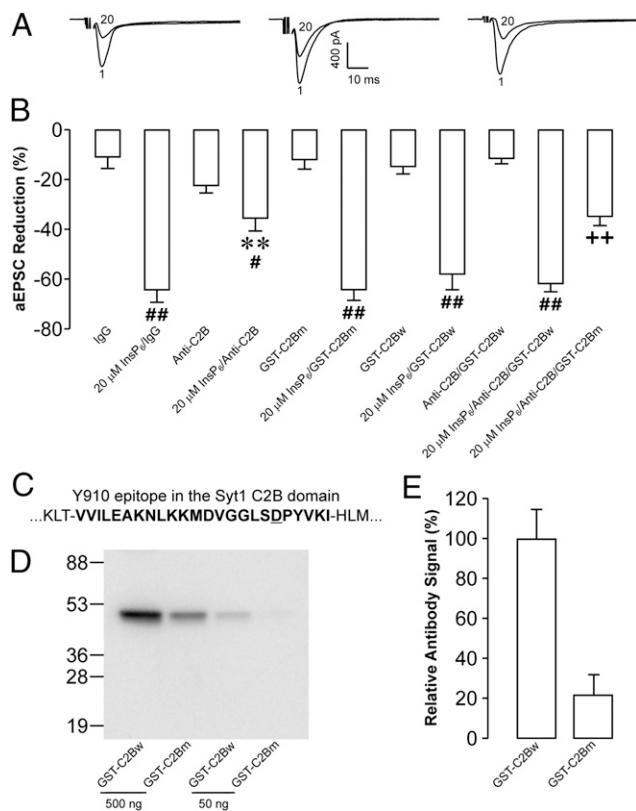


Fig. 4. Intracellular exposure to InsP₆ inhibits autaptic EPSCs (aEPSCs) via synaptotagmin-1 C2B domain. (A) Sample autaptic EPSC traces acquired in a neuron dialyzed with 20 μM InsP₆ plus nonimmune rabbit IgG (Left), a neuron subjected to internal exposure to 20 μM InsP₆ plus a polyclonal rabbit antibody against synaptotagmin-1 C2B domain (Anti-C2B) (Center), and a neuron subjected to dialysis of 20 μM InsP₆ in combination with Anti-C2B and GST-C2Bw (Right). Numbers indicate the time (min) when autaptic EPSCs were registered after forming the whole-cell configuration. (B) Summary graph shows that Anti-C2B codialyzed with InsP₆ (20 μM InsP₆/Anti-C2B, n = 9) produces significant attenuation of the InsP₆-induced inhibition of autaptic EPSCs compared with InsP₆ plus nonimmune IgG (20 μM InsP₆/IgG, n = 7; P < 0.01). Anti-C2B (n = 10) in the absence of InsP₆ only marginally reduces autaptic EPSCs compared with IgG (n = 9; P = 0.054). Importantly, preabsorption of Anti-C2B with GST-C2Bw (20 μM InsP₆/Anti-C2B/GST-C2Bw, n = 13) but not with GST-C2Bm (20 μM InsP₆/Anti-C2B/GST-C2Bm, n = 7) fully masks the effect of Anti-C2B on the InsP₆-induced inhibition of autaptic EPSCs. Anti-C2B preabsorbed with GST-C2Bw (Anti-C2B/GST-C2Bw, n = 11) produces no significant alteration in autaptic EPSCs in the absence of InsP₆. There is no significant difference in the InsP₆-induced inhibition of autaptic EPSCs between 20 μM InsP₆/IgG, 20 μM InsP₆/GST-C2Bm (n = 14), 20 μM InsP₆/GST-C2Bw (n = 8), and 20 μM InsP₆/Anti-C2B/GST-C2Bw. Like IgG, GST-C2Bm (n = 8) or GST-C2Bw (n = 8) on its own only slightly decreases aEPSCs. #P < 0.05 and ##P < 0.01 vs. corresponding treatments in the absence of InsP₆; **P < 0.01 vs. 20 μM InsP₆/IgG and 20 μM InsP₆/anti-C2B/GST-C2Bw; +++P < 0.01 vs. 20 μM InsP₆/anti-C2B/GST-C2Bw. (C) Sequence of the Y940 peptide epitope with underlining of the only residue in the epitope sequence that is altered in the mutant C2B domain. Thus, the antibody must primarily react with the exposed top loop 1 of the Ca²⁺-binding site of the C2B-domain because a single amino acid substitution in this loop severely impairs the antibody reactivity. (D) Representative immunoblot of the indicated amounts of purified WT and mutant (Mut) C2B domains probed with Y940 antibody and visualized with ¹²⁵I-labeled secondary antibodies and autoradiography. (E) Quantification of the reactivity of Y940 antibody with WT and mutant C2B domains using ¹²⁵I-labeled secondary antibodies and phosphorimager detection shows that the synaptotagmin-1 C2B domain antibody Y940 reacts more strongly with WT than Ca²⁺-binding site mutant C2B-domain (n = 3 independent experiments). pA, picoampere.

ulatory processes of RRP size and replenishment rate in InsP₆ inhibition on autaptic EPSCs suggests that intracellular InsP₆ may act on postsynaptic ionotropic glutamate receptors and/or on the final step of exocytosis, namely, fusion at presynaptic terminals.

The possibility for intracellular InsP₆ to inhibit autaptic EPSCs via postsynaptic ionotropic glutamate receptors has been ruled out by the following evidence. Whole-cell currents evoked by the nonselective glutamate receptor agonist glutamate as well as the selective ionotropic glutamate receptor agonists AMPA, NMDA, and kainite behave more or less the same in autapse-lacking neurons either dialyzed or not dialyzed with InsP₆. This confirmed that intracellular InsP₆ does not act on postsynaptic ionotropic glutamate receptors to inhibit EPSCs.

The fact that neither regulatory processes of RRP size and replenishment rate nor postsynaptic ionotropic glutamate receptors mediated InsP₆ inhibition on autaptic EPSCs made us consider the final step of exocytosis, namely, fusion. The fusion step is highly regulated by synaptotagmin-1. This abundant synaptic

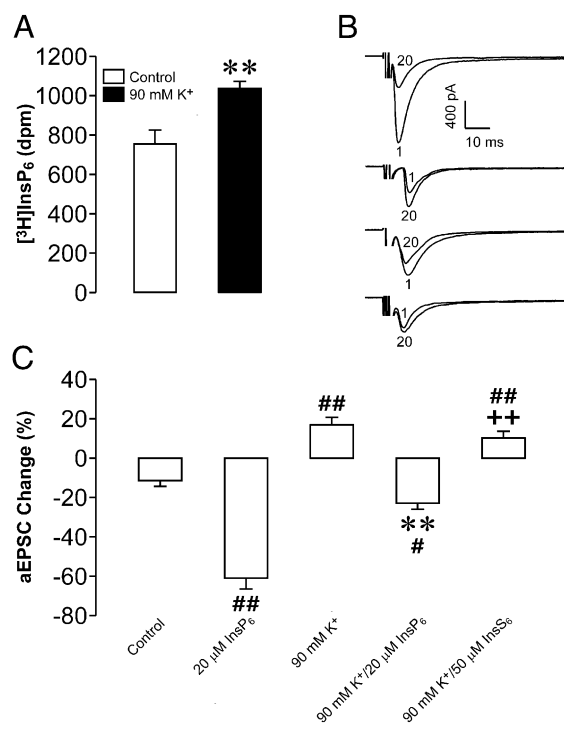


Fig. 5. K⁺ depolarization increases endogenous levels of InsP₆ and diminishes inhibition of exogenous InsP₆ on autaptic EPSCs. (A) Depolarization with 90 mM KCl for 1 min (n = 6) induces a significant increase in [³H]InsP₆ levels in hippocampal cultures labeled with [³H]inositol (30 μCi/mL) for 3 d. **P < 0.01 vs. control (n = 6). (B) Sample autaptic EPSC (aEPSC) traces acquired in a neuron not subjected to prior K⁺ depolarization with a recording pipette containing 20 μM InsP₆ (Top), a neuron subjected to prior K⁺ depolarization with a pipette containing no InsP₆ (Middle Upper), a neuron following K⁺ depolarization with a pipette containing 20 μM InsP₆ (Middle Lower), and a neuron exposed to prior K⁺ depolarization with a pipette containing 20 μM InsP₆ (Bottom). Numbers indicate the time (min) when autaptic EPSCs were registered after forming the whole-cell configuration. (C) Summary graph shows that intracellular exposure to 20 μM InsP₆ (n = 11) significantly reduces autaptic EPSCs in comparison to exposure to vehicle (control) (n = 11; P < 0.01). The InsP₆-induced reduction of autaptic EPSCs in neurons subjected to prior K⁺ depolarization (n = 12) is significantly less than that in those without prior K⁺ depolarization (P < 0.01). Neurons following K⁺ depolarization even display an appreciable increase in autaptic EPSCs in the absence (n = 14) and presence (n = 13) of 20 μM InsP₆. #P < 0.05 and ##P < 0.01 vs. control; **P < 0.01 vs. 20 μM InsP₆; +++P < 0.01 vs. 90 mM K⁺/20 μM InsP₆. dpm, disintegrations per minute; pA, picoampere.

size and replenishment rate, quantified by puffing hypertonic sucrose, when internally exposed to InsP₆. The bypass of reg-

vesicle membrane protein consists of a short N-terminal intravesicular sequence, a single transmembrane region, and two cytoplasmic repeats with homology to the C2 domain of protein kinase C (i.e., the C2A and C2B domains) (27). Both the C2A and C2B domains are essential in neurotransmission (27). It is believed that the C2A domain functions as a Ca^{2+} sensor, whereas the C2B domain binds to inositol polyphosphates, including $InsP_6$, with high affinity irrespective of the presence of Ca^{2+} (27). Therefore, we concentrated on the C2B domain of synaptotagmin-1 to understand the mechanisms whereby $InsP_6$ inhibits autaptic EPSCs in hippocampal neurons. Our results revealed that the $InsP_6$ -induced inhibition of autaptic EPSCs was significantly abrogated by coapplied Anti-C2B. Importantly, Anti-C2B preabsorbed with GST-C2Bw but not GST-C2Bm fully lost its capacity to abrogate the $InsP_6$ -induced inhibition of autaptic EPSCs.

The mitigation of the effect of $InsP_6$ by the C2B domain antibody is likely attributable to masking of $InsP_6$ -binding sites on native synaptotagmin I C2B domain by Anti-C2B, as shown by the neutralization of the C2B domain antibody activity by recombinant C2B domain protein. Strikingly, only WT but not mutant C2B domain protein was able to neutralize the C2B domain antibody. Because the mutation is localized to the Ca^{2+} -binding site of the C2B domain, this result reveals that $InsP_6$ must act on the Ca^{2+} -binding site of synaptotagmin-1, consistent with biochemical data that $InsP_6$ inhibits Ca^{2+} -dependent membrane interactions of synaptotagmin C2 domains (28). GST-C2Bw can also have a dominant negative activity on the native synaptotagmin-1-mediated exocytosis (20). However, such an activity requires a higher concentration of GST-C2B (20). Therefore, intracellular application of GST-C2B at a relatively lower concentration in the absence and presence of $InsP_6$ in the present work did not produce an appreciable effect on autaptic EPSCs. These results, taken together with our aforementioned observations, demonstrate that $InsP_6$ suppresses excitatory neurotransmission via inhibition of presynaptic synaptotagmin-1 C2B domain-mediated fusion rather than via deceleration of synaptic vesicle trafficking and inactivation of postsynaptic ionotropic glutamate receptors. This is consistent with the fact that inositol polyphosphates act at the C2B domain of synaptotagmin-1 to attenuate neurotransmitter release from squid giant presynaptic terminals (29).

Obviously, evidence for the physiological relevance of exogenous $InsP_6$ -induced inhibition of excitatory neurotransmission should be acquired. Therefore, we examined endogenous levels

of $InsP_6$ and their effect on exogenous $InsP_6$ -induced inhibition of autaptic EPSCs in cultured hippocampal neurons following K^+ depolarization. Our observation shows that K^+ depolarization significantly elevates endogenous levels of $InsP_6$ and elevated endogenous $InsP_6$ effectively occludes the inhibition of exogenous $InsP_6$ on autaptic EPSCs in depolarized neurons. It has been demonstrated that depolarization with high K^+ dramatically increases $InsP_6$ levels in cerebellar granule neurons (30). Our previous work has also revealed that electrically evoked convulsive seizure significantly increases $InsP_6$ levels in several brain regions, including hippocampus (13 μM in control hippocampi and 22 μM in hippocampi subjected to electrically evoked convulsive seizure) (13). Our observations, together with the findings obtained by others, provide strong evidence that elevated $InsP_6$ in activated neurons serves as a unique negative feedback signal to inhibit excitatory neurotransmission. The hippocampus relies on adequate neurotransmission for higher brain functions, such as learning and memory (31, 32). Abnormal changes in hippocampal neurotransmission are associated with a series of neurological and psychiatric disorders, such as epilepsy, schizophrenia, and Alzheimer's disease (33). Therefore, $InsP_6$ -mediated negative feedback control of hippocampal excitatory neurotransmission plays an important role in maintenance of normal brain function.

Methods

Experimental details are described in *SI Methods*. Briefly, dissociated hippocampal neurons from 18-d pregnant Sprague-Dawley rats (B & K Universal AB) were cultured for 11–16 d. Conventional whole-cell patch-clamp recordings were performed on pyramidal-type cells with an Axopatch 200B amplifier (Molecular Devices). Hippocampal cultures were labeled with [3H] inositol (30 $\mu Ci/mL$) for 3 d. [3H] $InsP_6$ was analyzed using HPLC (34). Data are presented as means \pm SEM. Statistical significance was evaluated by an unpaired Student *t* test or one-way ANOVA, followed by a least significant difference test.

ACKNOWLEDGMENTS. This work was supported by Berth von Kantzow's Foundation, EuroDia (Grant FP6-518153), the European Foundation for the Study of Diabetes, the Family Erling-Persson Foundation, Fredrik and Ingrid Thuring's Foundation, the Karolinska Institutet, the Knut and Alice Wallenberg Foundation, Magnus Bergvall's Foundation, the Novo Nordisk Foundation, Skandia Insurance Company, the Stichting af Jochnick Foundation, the Strategic Research Program in Diabetes at the Karolinska Institutet, the Swedish Alzheimer Association, the Swedish Diabetes Association, the Swedish Foundation for Strategic Research, the Swedish Research Council, the Swedish Society of Medicine, the Torsten and Ragnar Söderberg Foundation, the Consortium of In Vivo Imaging of Beta-cell Receptors by Applied Nano Technology (Grant FP7-228933-2), and Åke Wiberg's Foundation.

- Yang SN, Berggren PO (2006) The role of voltage-gated calcium channels in pancreatic β -cell physiology and pathophysiology. *Endocr Rev* 27:621–676.
- Shears SB (1996) Inositol pentakis- and hexakisphosphate metabolism adds versatility to the actions of inositol polyphosphates. Novel effects on ion channels and protein traffic. *Subcell Biochem* 26:187–226.
- Fukuda M, Mikoshiba K (1997) The function of inositol high polyphosphate binding proteins. *Bioessays* 19:593–603.
- Tsui MM, York JD (2010) Roles of inositol phosphates and inositol pyrophosphates in development, cell signaling and nuclear processes. *Adv Enzyme Regul* 50:324–337.
- Montpetit B, et al. (2011) A conserved mechanism of DEAD-box ATPase activation by nucleoporins and $InsP_6$ in mRNA export. *Nature* 472:238–242.
- Larsson O, et al. (1997) Inhibition of phosphatases and increased Ca^{2+} channel activity by inositol hexakisphosphate. *Science* 278:471–474.
- Yang SN, Berggren PO (2005) β -cell Ca_v channel regulation in physiology and pathophysiology. *Am J Physiol Endocrinol Metab* 288:E16–E28.
- Høy M, et al. (2002) Inositol hexakisphosphate promotes dynamin I-mediated endocytosis. *Proc Natl Acad Sci USA* 99:6773–6777.
- Høy M, Berggren PO, Gromada J (2003) Involvement of protein kinase C- ϵ in inositol hexakisphosphate-induced exocytosis in mouse pancreatic beta-cells. *J Biol Chem* 278:35168–35171.
- Efanov AM, Zaitsev SV, Berggren PO (1997) Inositol hexakisphosphate stimulates non- Ca^{2+} -mediated and primes Ca^{2+} -mediated exocytosis of insulin by activation of protein kinase C. *Proc Natl Acad Sci USA* 94:4435–4439.
- Parent A, Quirion R (1994) Differential localization and pH dependency of phosphoinositide 1,4,5- IP_3 , 1,3,4,5- IP_4 , and IP_6 receptors in rat and human brains. *Eur J Neurosci* 6:67–74.
- Vallejo M, Jackson T, Lightman S, Hanley MR (1987) Occurrence and extracellular actions of inositol pentakis- and hexakisphosphate in mammalian brain. *Nature* 330:656–658.
- Yang SN, et al. (2001) Inositol hexakisphosphate increases L-type Ca^{2+} channel activity by stimulation of adenylyl cyclase. *FASEB J* 15:1753–1763.
- Bekkers JM, Stevens CF (1991) Excitatory and inhibitory autaptic currents in isolated hippocampal neurons maintained in cell culture. *Proc Natl Acad Sci USA* 88:7834–7838.
- Rosenmund C, Stevens CF (1996) Definition of the readily releasable pool of vesicles at hippocampal synapses. *Neuron* 16:1197–1207.
- Stevens CF, Tsujimoto T (1995) Estimates for the pool size of releasable quanta at a single central synapse and for the time required to refill the pool. *Proc Natl Acad Sci USA* 92:846–849.
- Stevens CF, Wesseling JF (1999) Identification of a novel process limiting the rate of synaptic vesicle cycling at hippocampal synapses. *Neuron* 24:1017–1028.
- Geppert M, et al. (1994) Synaptotagmin I: A major Ca^{2+} sensor for transmitter release at a central synapse. *Cell* 79:717–727.
- Shin OH, Xu J, Rizo J, Südhof TC (2009) Differential but convergent functions of Ca^{2+} binding to synaptotagmin-1 C2 domains mediate neurotransmitter release. *Proc Natl Acad Sci USA* 106:16469–16474.
- Shin OH, et al. (2003) Sr^{2+} binding to the Ca^{2+} binding site of the synaptotagmin 1 C2B domain triggers fast exocytosis without stimulating SNARE interactions. *Neuron* 37:99–108.
- Fernandez I, et al. (2001) Three-dimensional structure of the synaptotagmin 1 C2B domain: Synaptotagmin 1 as a phospholipid binding machine. *Neuron* 32:1057–1069.
- Südhof TC (1995) The synaptic vesicle cycle: A cascade of protein-protein interactions. *Nature* 375:645–653.
- Rizzoli SO, Betz WJ (2005) Synaptic vesicle pools. *Nat Rev Neurosci* 6:57–69.

24. Südhof TC (2004) The synaptic vesicle cycle. *Annu Rev Neurosci* 27:509–547.
25. Stevens CF, Wesseling JF (1998) Activity-dependent modulation of the rate at which synaptic vesicles become available to undergo exocytosis. *Neuron* 21:415–424.
26. Goda Y, Südhof TC (1997) Calcium regulation of neurotransmitter release: Reliably unreliable? *Curr Opin Cell Biol* 9:513–518.
27. Rizo J, Südhof TC (1998) C₂-domains, structure and function of a universal Ca²⁺-binding domain. *J Biol Chem* 273:15879–15882.
28. Lu YJ, He Y, Sui SF (2002) Inositol hexakisphosphate (InsP6) can weaken the Ca²⁺-dependent membrane binding of C2AB domain of synaptotagmin I. *FEBS Lett* 527:22–26.
29. Fukuda M, et al. (1995) Role of the C2B domain of synaptotagmin in vesicular release and recycling as determined by specific antibody injection into the squid giant synapse preterminal. *Proc Natl Acad Sci USA* 92:10708–10712.
30. Sasakawa N, Nakaki T, Kakinuma E, Kato R (1993) Increase in inositol tris-, pentakis- and hexakisphosphates by high K⁺ stimulation in cultured rat cerebellar granule cells. *Brain Res* 623:155–160.
31. Kandel ER (2001) The molecular biology of memory storage: A dialogue between genes and synapses. *Science* 294:1030–1038.
32. Deng W, Aimone JB, Gage FH (2010) New neurons and new memories: How does adult hippocampal neurogenesis affect learning and memory? *Nat Rev Neurosci* 11:339–350.
33. Small SA, Schobel SA, Buxton RB, Witter MP, Barnes CA (2011) A pathophysiological framework of hippocampal dysfunction in ageing and disease. *Nat Rev Neurosci* 12:585–601.
34. Yu J, et al. (2003) Cytosolic multiple inositol polyphosphate phosphatase in the regulation of cytoplasmic free Ca²⁺ concentration. *J Biol Chem* 278:46210–46218.